Bivariate Fisher–Snedecor $\mathcal{F}$ Distribution with Arbitrary Fading Parameters

Weijun Cheng(✉), Xianmeng Xu, Xiaoting Wang, and Xiaohan Liu

School of Information Engineering, Minzu University of China, Beijing, People's Republic of China
weijuncheng@muc.edu.cn

Abstract. A bivariate Fisher–Snedecor $\mathcal{F}$ composite distribution with arbitrary fading parameters (not necessary identical) is presented in this paper. We derive novel theoretical formulations of the statistical characteristics for the correlated $\mathcal{F}$ composite fading model, which include the joint probability density function, the joint cumulative distribution function, the joint moments and the power correlation coefficient. Capitalizing on the joint cumulative distribution function, the bit error rate for binary digital modulation systems and the outage probability of a correlated dual-branch selection diversity system, and the level crossing rate and the average fade duration of a sampled Fisher-Snedecor $\mathcal{F}$ composited fading envelope are obtained, respectively. Finally, we employ numerical and simulation results to demonstrate the validity of the theoretical analysis under various correlated fading and shadowing scenarios.

Keywords: Fisher–Snedecor $\mathcal{F}$ distribution · Correlated composite fading · Selection diversity · Second-order statistics

1 Introduction

More recently, the Fisher-Snedecor $\mathcal{F}$ fading channel model has been paid great attention in the performance evaluation of wireless digital communication systems [1–9]. This channel model was firstly presented in [1]. It accurately describes the composite impacts of both shadowing components and multipath components on the faded signal, where shadowing components follow inverse Nakagami-m distribution and multipath components follow Nakagami-m distribution. Compared to generalized-K (Nakagami-Gamma) composite fading model, the authors in [1] showed that under non-LOS (NLOS) and line-of-sight (LOS) environments the Fisher composite fading model has a better fit to experimental channel measurements, such as wireless body area networks and device-to-device (D2D) communications. Furthermore, this fading model can reduce to one-sided Gaussian, Rayleigh and Nakagami-m as special cases in the absence of shadowing components. In addition, its other advantage is that the closed-form expressions of its statistical characteristics are more tractable and simpler than those of generalized-K distribution.

The authors in [2] gave the theoretical formulations of the sum of independent and non-identically distributed (i.n.i.d.) random variables (RVs) following Fisher-Snedecor $\mathcal{F}$ distribution and applied them in maximal ratio combining (MRC) receivers. The

H. Gao et al. (Eds.): TridentCom 2019, LNICST 309, pp. 107–119, 2020.
https://doi.org/10.1007/978-3-030-43215-7_8

performance of physical layer security was investigated over $\mathcal{F}$ composite fading channels in [3]. The authors in [1] further studied the achievable channel capacity and energy detection-based spectrum sensing in Fisher-Snedecor $\mathcal{F}$ fading in [4] and [5], respectively. In [6], the performance of the selection combining (SC) scheme with i.n.i.d branches over $\mathcal{F}$ composite fading channels was analyzed. Authors in [7] considered the ergodic capacity of several adaptive transmission strategies and obtained asymptotic and exact representations in Fisher–Snedecor $\mathcal{F}$ fading channels. The effective rate (ER) analysis of multiple-input single-output (MISO) systems was presented in i.n.i.d. and i.i.d. Fisher-Snedecor $\mathcal{F}$ fading channels in [8]. In [9], the symbol error rate (SER) of M-ary quadrature amplitude modulation (M-QAM) and M-ary pulse amplitude modulation (M-PAM), and the average capacity were derived and evaluated in Fisher-Snedecor $\mathcal{F}$ fading channels.

Although the MRC and SC systems over Fisher-Snedecor $\mathcal{F}$ composite fading channel have been investigated in [2] and [6], the authors only considered the i.n.i.d. fading environments. When the distance between antennas is less than 0.38λ in a diversity system, the received signals could cause correlated each other and lead to a decrease of the diversity gain, where λ is the wavelength of the carrier. To be specific, this signal correlation usually occurs in relatively small size mobile equipment because the space between their diversity branches can be too close to keep the received signals independent. Thus, the correlated analysis of the received signals are crucial in the performance evaluation of the diversity received systems. Up to now, the correlated distribution in wireless communication diversity systems has been studied extensively in the open research works. Nevertheless, most of them only considered either the correlated small scale fading or the correlated shadowing, such as [10, 11]. For correlated multipath and shadowing composite distributions, only a few papers have been involved. Based on a gamma shadowing distribution, the correlated K distribution (Rayleigh-Gamma) and generalized-K distribution were investigated in [12] and [13], respectively. In [14] and [15], the outage probability of SC receivers was studied over correlated Weibull-gamma fading channels with identical and non-identical fading conditions, respectively. By using an inverse Gaussian shadowing model, bivariate $\mathcal{G}$ (Rayleigh-inverse Gaussian) fading distribution has been proposed and employed to the dual-branch SC and MRC diversity receivers in [16]. In [17], the authors obtained the statistical properties of bivariate Nakagami-lognormal distribution and discussed the correlation properties under micro- and macro-diversity environments.

To the best of the authors' knowledge, the correlated (bivariate) Fisher–Snedecor $\mathcal{F}$ channel model has not been considered in the published research works. Motivated by the above observation, we study the bivariate Fisher–Snedecor $\mathcal{F}$ composite distribution with not necessary identical fading parameters and its applications in this paper. The statistical characteristics of correlated Fisher–Snedecor $\mathcal{F}$ composite distribution including the bivariate probability density function (PDF), the bivariate cumulative distribution function (CDF) and the joint moments are derived. Capitalizing on the joint CDF, the bit error rate (BER) of binary digital modulation schemes and the outage probability (OP) for a correlated dual-branch SC receiver, the average fade duration (AFD) and the level crossing rate (LCR) of a sampled Fisher-Snedecor $\mathcal{F}$ composited fading envelope are also given, respectively. Finally, we evaluate the validity of the

performance analysis by using numerical analysis and simulation under various correlated fading and shadowing scenarios.

The remainder of this paper is organized as follows: the closed-form expressions of statistical characteristics of the bivariate Fisher–Snedecor $\mathcal{F}$ composite distribution are derived in Sect. 2. The performance analysis of a correlated dual-branch SC receiver is presented in Sect. 3, and Sect. 4 gives the second-order statistics of a sampled composited fading envelope. Numerical and simulation analysis are shown and discussed in Sects. 5 and 6 outlines the main conclusions.

2 Statistical Characteristics

Let X_i (i = 1, 2) be the channel fading envelopes of Nakagami-m processes, and the bivariate (joint) PDF between X_1 and X_2 given from [10, eq. (12)] as

$$f_{X_1,X_2}(x_1,x_2) = 4(1-\rho_N)^{m_2}\sum_{k=0}^{\infty}\frac{(m_1)_k\rho_N^k}{k!}{}_1F_1[m_2-m_1,m_2+k;\frac{\rho_N m_2 x_2^2}{Y_2(1-\rho_N)}] \times \prod_{i=1}^{2}\left[\frac{m_i}{Y_i(1-\rho_N)}\right]^{m_i+k}\frac{x_i^{2(m_i+k)-1}}{\Gamma(m_i+k)}\exp\left[-\frac{m_i x_i^2}{(1-\rho_N)Y_i}\right] \quad (1)$$

where $m_2 > m_1 \geq 1/2$ is the Nakagami-m shaping parameter, Y_i is the average fading power $\mathrm{Y}_i = \mathbb{E}\left[X_i^2\right]$ with $\mathbb{E}[\cdot]$ denoting expectation, and ρ_N denotes the power correlation coefficient between X_1^2 and X_2^2. Furthermore, ${}_1F_1(\cdot;\cdot;\cdot)$ is the confluent hypergeometric function defined in [18, eq. (9.210/1)], $(x)p$ is the Pochhammer's symbol defined in [18, p. xliii], $(x)_p = \Gamma(x+p)/\Gamma(x)$, with $p \in \mathbb{N}$, and $\Gamma(\cdot)$ is the gamma function in [18, eq. (8.310/1)].

In composite fading environments, Y_i slowly varies when small scale fading is superimposed on shadowing, and its root-mean-square (rms) can be considered as a random variable following the inverse Nakagami-m distribution. Based on the proposed signal model in [1], $\mathrm{Y}_i = w_i^2\Omega_i$, where w_i is inverse Nakagami-m random variable, $\Omega_i = \mathbb{E}\left[R_i^2\right]$ denotes the mean power of the composite signal envelope R_i, then the PDF in (1) is conditioned on w_i. To model the inverse Nakagami-m distribution, we let the parameter $w_i = 1/r_i$, where r_i follows Nakagami-m distribution defined in [10, eq. (12)]. By utilizing a change of random variables, the joint PDF of inverse Nakagami-m distribution can be obtained as

$$f_{\mathrm{W}_1,\mathrm{W}_2}(w_1,w_2) = 4(1-\rho_G)^{n_2}\sum_{l=0}^{\infty}\frac{(n_1)_l\rho_G^l}{l!}{}_1F_1[n_2-n_1,n_2+l;\frac{\rho_G n_2 w_2^{-2}}{1-\rho_G}] \times \prod_{j=1}^{2}\left[\frac{n_j}{1-\rho_G}\right]^{n_j+l}\frac{w_j^{-2(n_j+l)-1}}{\Gamma(n_j+l)}\exp\left[-\frac{n_j w_j^{-2}}{1-\rho_G}\right] \quad (2)$$

where $n_2 > n_1 \geq 1/2$ is the inverse Nakagami-m shaping parameter, ρ_G denotes the power correlation coefficient between w_1^2 and w_2^2. In this paper, we set scale parameter, Ω_s, equal to unity.

In [1], the PDF of Fisher–Snedecor $\mathcal{F}$ composite envelopes is obtained by averaging the conditional PDF of the Nakagami-m process over the random variation of the rms signal power. Therefore, the joint PDF of bivariate Fisher–Snedecor $\mathcal{F}$ composite distribution is written as

$$f_{R_1,R_2}(r_1,r_2) = \int_0^\infty \int_0^\infty f_{Y_1|W_1,Y_2|W_2}(r_1|w_1,r_2|w_2) f_{W_1,W_2}(w_1,w_2) dw_1 dw_2 \tag{3}$$

By substituting (1) and (2) in (3), and using [19, eq. (55)], the joint PDF of bivariate Fisher–Snedecor $\mathcal{F}$ distribution can be derived, after some algebraic manipulations, as

$$\begin{aligned} f_{R_1,R_2}(r_1,r_2) = & \sum_{k=0}^{\infty}\sum_{l=0}^{\infty} \frac{4(m_1)_k \rho_N^k (n_1)_l \Theta \rho_G^l}{k!l!B(m_1+k,n_1+l)B(m_2+k,n_2+l)} \\ & \times \frac{\beta_1^{m_1+k}\beta_2^{m_2+k} r_1^{2(m_1+k)-1} r_2^{2(m_2+k)-1}}{\left(1+\beta_1 r_1^2\right)^{\lambda_1}\left(1+\beta_2 r_2^2\right)^{-\lambda_2}} \\ & \times F_2\left[\lambda_2; m_2-m_1, n_2-n_1; m_2+k, n_2+l; \frac{\rho_N \beta_2 r_2^2}{\beta_2 r_2^2+1}, \frac{\rho_G}{\beta_2 r_2^2+1}\right] \end{aligned} \tag{4}$$

where $\beta_i = m_i(1-\rho_G)/(n_i(1-\rho_N)\Omega_i), (i=1,2), B(\cdot,\cdot)$ is the Beta function defined in [18, eq. (8.384.1)], $F_2[\cdot]$ is the Appell Hypergeometric function defined in [18, eq. (9.180.2)], $\lambda_1 = m_1+k+n_1+l$, $\lambda_2 = m_2+k+n_2+l$, $\Theta = (1-\rho_N)^{m_2}(1-\rho_G)^{n_2}$.

To achieve a closed-form representation of joint CDF, we use the infinite series expressions of the Appell's function in [18, eq. (9.180.2)]. Based on (4), the corresponding joint CDF of R_1 and R_2 can be given by

$$\begin{aligned} F_{R_1,R_2}(r_1,r_2) = & \int_0^{r_1}\int_0^{r_2} f_{R_1,R_2}(r_1,r_2) dr_1 dr_2 \\ = & \sum_{k=0}^{\infty}\sum_{l=0}^{\infty}\sum_{i=0}^{\infty}\sum_{j=0}^{\infty} \frac{\rho_N^{k+i}\rho_G^{l+j}\Theta\beta_1^{m_1+k}\beta_2^{m_2+k+i}}{i!j!k!l!\Gamma(m_1)\Gamma(n_1)} \\ & \times \frac{(m_2-m_1)_i (n_2-n_1)_j \Gamma(\lambda_1) r_1^{2(m_1+k)} r_2^{2(m_2+k+i)}}{B(m_2+k+i,n_2+l+j)(m_1+k)(m_2+k+i)} \\ & \times {}_2F_1[\lambda_1, m_1+k; m_1+k+1; -\beta_1 r_1^2] \\ & \times {}_2F_1[\lambda_2+i+j, m_2+k+i; m_2+k+i+1; -\beta_2 r_2^2] \end{aligned} \tag{5}$$

where ${}_2F_1[\cdot]$ is the Gauss hypergeometric function in [18, eq. (9.100)].

The joint central moments of the bivariate Fisher–Snedecor $\mathcal{F}$ composite distribution can be obtained as

$$\begin{aligned}\mu_{R_1,R_2}(q_1,q_2) =& E[r_1^{q_1} r_2^{q_2}] \\ =& \int_0^\infty \int_0^\infty r_1^{q_1} r_2^{q_2} f_{R_1,R_2}(r_1,r_2) dr_1 dr_2\end{aligned} \tag{6}$$

By substituting (4) into (6), and employing [18, eq. (3.194.3)] and the identities [18, eqs. (9.180.1) and (9.182.11)], after some mathematical manipulations, we have

$$\begin{aligned}\mu_{R_1,R_2}(q_1,q_2) =& \frac{B(m_1+q_1/2, n_1-q_1/2)\,{}_2F_1[-q_2/2, -q_1/2; m_2; \rho_N]}{\left(B(m_2+q_2/2, n_2-q_2/2)\,{}_2F_1[q_2/2, q_1/2; n_2; \rho_G]\right)^{-1}} \\ &\times \frac{(n_1\Omega_1/m_1)^{q_1/2}(n_2\Omega_2/m_2)^{q_1/2}}{B(m_1,n_1)B(m_2,n_2)}\end{aligned} \tag{7}$$

By definition, the power correlation coefficient of R_1^2 and R_2^2 can be expressed as

$$\rho \triangleq \frac{\mathrm{cov}(r_1^2, r_2^2)}{\sqrt{\mathrm{var}(r_1^2)}\sqrt{\mathrm{var}(r_2^2)}} = \frac{\mathrm{E}[r_1^2 r_2^2] - \mathrm{E}[r_1^2]\mathrm{E}[r_2^2]}{\sqrt{\mathrm{E}[r_1^4] - \mathrm{E}^2[r_1^2]}\sqrt{\mathrm{E}[r_2^4] - \mathrm{E}^2[r_2^2]}} \tag{8}$$

where $\mathrm{E}(r_i^q) = \frac{B(m_i+q/2, n_i-q/2)}{B(m_i,n_i)(m_i/n_i\Omega_i)^{q/2}}$ is given in [1], $i = 1, 2$.

Then, substituting (7) into (8) and after some straightforward simplifications, the correlation coefficient can be yielded as

$$\rho \triangleq \frac{{}_2F_1(-1,-1;m_2;\rho_G)\,{}_2F_1(1,1;n_2;\rho_N) - 1}{\sqrt{\frac{(m_1+n_1-1)(m_2+n_2-1)}{m_1 m_2 (n_1-2)(n_2-2)}}} \tag{9}$$

3 Dual-Branch SC Diversity Receiver

In this paper, we consider a correlated dual-branch SC receiver over Fisher–Snedecor $\mathcal{F}$ composite environments. Its equivalent baseband received signal at the ith ($i = 1, 2$) antenna can be given by $r_i = ag_i + n_i$, in which a denotes the complex transmitted symbol with average energy $E_a = \mathbb{E}[|a|^2]$, n_i denotes the complex AWGN (additive white Gaussian noise) with N_0 (single sided power spectral density) which is supposed identical and uncorrelated to two branches, and g_i denotes the complex channel gain with its magnitude $R_i = |g_i|$ following a Fisher–Snedecor $\mathcal{F}$ distribution. Furthermore,

the general assumptions are made that only the channel fading magnitude has effects on the received signal and the phase can be accurately estimated, similar as in [13]. The instantaneous SNR (signal-to-noise ratio) per received symbol is written as $\gamma_i = R_i^2 E_a/N_0$, its average SNR can be given as $\bar{\gamma}_i = \mathbb{E}\left[R_i^2\right] E_a/N_0 = \Omega_i E_a/N_0$. In the following, we will give the OP and the BER analysis of the correlated dual-branch SC diversity system over Fisher–Snedecor $\mathcal{F}$ composite fading, respectively.

3.1 Outage Probability

For a SC receiver, the instantaneous output SNR can be expressed $\gamma_{SC} = \max(\gamma_1, \gamma_2)$, its corresponding CDF can be written as $F_{\gamma_{SC}}(\gamma) = F_{\gamma_1,\gamma_2}(\gamma,\gamma)$ in [20]. By making use of (5) and this equation, and carrying out a simple transformation of variables, we obtain the close-form expressions of $F_{\gamma_{SC}}(\gamma)$ over correlated Fisher–Snedecor $\mathcal{F}$ composite fading as follows

$$\begin{aligned} F_{\gamma_{SC}}(\gamma) = & \sum_{k=0}^{\infty}\sum_{l=0}^{\infty}\sum_{i=0}^{\infty}\sum_{j=0}^{\infty} \frac{\rho_N^{k+i}\rho_G^{l+j}\Theta\alpha_1^{m_1+k}\alpha_2^{m_2+k+i}}{k!l!i!j!\Gamma(m_1)\Gamma(n_1)} \\ & \times \frac{(m_2-m_1)_i(n_2-n_1)_j\Gamma(\lambda_1)\gamma^{\lambda_3}}{B(m_2+k+i,n_2+l+j)(m_1+k)(m_2+k+i)} \\ & \times {}_2F_1[\lambda_1, m_1+k; m_1+k+1; -\alpha_1\gamma] \\ & \times {}_2F_1[\lambda_2+i+j, m_2+k+i; m_2+k+i+1; -\alpha_2\gamma] \end{aligned} \tag{10}$$

where $\alpha_i = m_i(1-\rho_G)/n_i(1-\rho_N)\bar{\gamma}_i$, $\lambda_3 = m_1 + 2k + m_2 + i$.

The OP is the probability that the instantaneous output SNR of SC falls below a given outage threshold γ_{th} in [20]. Utilizing (10), we can obtain the OP by using γ_{th} instead of γ as Pout $= F_{\gamma_{SC}}(\gamma_{th})$.

3.2 Bit Error Rate

By using (10) and the Eq. (12) in [21], we can obtain the average BER as follows

$$\bar{P}_e = \frac{q^p}{2\Gamma(p)}\int_0^{\infty} \exp(-q\gamma_{SC})\gamma_{SC}^{p-1}F_{\gamma_{SC}}(\gamma_{SC})d\gamma_{SC} \tag{11}$$

where the parameters p and q for different digital modulation systems has been given in [22]. Specifically, $p = 1$, $q = 1$ for DPSK (differential phase shift keying), $p = 0.5$, $q = 1$ for BPSK (binary phase shift keying) and BFSK (binary frequency shift keying) is represented by $p = 0.5$ and $q = 0.5$.

Substituting (10) into (11), and using [23, eqs. (12) and (9)] along with some mathematical manipulations, (11) can be rewritten as

$$P_e = \sum_{k=0}^{\infty}\sum_{l=0}^{\infty}\sum_{i=0}^{\infty}\sum_{j=0}^{\infty}\frac{q^p \rho_N^{k+i}\rho_G^{l+j}\Theta\alpha_1^{m_1+k}\alpha_2^{m_2+k+i}}{2\Gamma(p)i!j!k!l!q^{\lambda_3+p}} \times \frac{(m_2-m_1)_i(n_2-n_1)_j}{\Gamma(m_1)\Gamma(n_1)\Gamma(m_2+k+i)\Gamma(n_2+l+j)} \times G_{1,0:2,2:2,2}^{0,1:1,2:1,2}\left[\begin{matrix}0.5-\lambda_3 \\ -\end{matrix}\middle|\begin{matrix}1-\lambda_1,1-(m_1+k) \\ 0,-(m_1+k)\end{matrix}\middle|\begin{matrix}1-\lambda_2+i+j,1-(m_2+k+i) \\ 0,-(m_2+k+i)\end{matrix}\middle|\frac{\alpha_1}{q},\frac{\alpha_2}{q}\right] \tag{12}$$

where $G[\cdot|\cdot|\cdot\,|\cdot,\cdot]$ is a bivariate Merjer G-function which is used in [23]. Noted that a Mathematical code that is provided in [23] is available to calculate it.

4 Level Crossing Rate and Average Fade Duration

As two important examples, The LCR and AFD are often applied to characterize higher-order statistics of the received signal envelope in small scale multipath and/or large scale shadowing environments. They are very helpful to design and select error control techniques and diversity systems since they can provide useful information about the burst error statistics. The former denotes the expected rate at which the fading envelope crosses a specified threshold level in a positive (or negative) direction, while the latter is defined as the average period of time which the envelope stays below this threshold level. Traditionally, the joint PDF of the continuous fading envelop and its time derivative has been employed to calculate them. In [24], the authors proposed an alternative analytical approach that the AFD and the LCR can be obtained based on the CDF and the bivariate CDF of a sampled random envelope. Recently this approach has been used to evaluate the LCR and the AFD in a Rician shadowed fading channel in [25]. In [24], the LCR of a sampled random envelope is written as

$$LCR(\mu) = \frac{\Pr\{R_1 < \mu, R_2 > \mu\}}{T_s} \tag{13}$$

where $R_1 \triangleq R(t)$ and $R_2 \triangleq R(t+Ts)$ are correlated and identical random variables, $R(t)$ is the continuous time envelope, μ is a specified threshold level and Ts denotes the sampling period. Moreover, the CDF of R_1 and R_2 is given as $F_R(x) \triangleq F_{R_1}(x) \triangleq F_{R_2}(x)$. Therefore, we can express the compact form of the LCR by using the bivariate CDF of R_1 and R_2 and the marginal CDF of R_1 as follows

$$LCR(\mu) = \frac{F_{R_1}(\mu) - F_{R_1,R_2}(\mu,\mu)}{T_s} \tag{14}$$

where $F_{R_1}(\mu)$ can been found in [1]. Substituting (5) into (14), the LCR can be obtained as

$$
\begin{aligned}
LCR(\mu) = & \frac{m_1^{m_1-1}\mu^{2m_1}}{B(m_1,n_1)(n_1\Omega_1)^{m_1}T_s}\,{}_2F_1\left[m_1+n_1,m_1;m_1+1;-\frac{m_1\mu^2}{n_1\Omega_1}\right] \\
& - \sum_{k=0}^{\infty}\sum_{l=0}^{\infty}\sum_{i=0}^{\infty}\sum_{j=0}^{\infty}\frac{\rho_N^{k+i}\rho_G^{l+j}\Theta\beta_1^{m_1+k}\beta_2^{m_2+k+i}}{i!j!k!l!\Gamma(m_1)\Gamma(n_1)T_s} \\
& \times \frac{(m_2-m_1)_i(n_2-n_1)_j\Gamma(\lambda_1)\mu^{2\lambda_3}}{B(m_2+k+i,n_2+l+j)(m_1+k)(m_2+k+i)} \\
& \times {}_2F_1\left[\lambda_1,m_1+k;m_1+k+1;-\beta_1\mu^2\right] \\
& \times {}_2F_1\left[\lambda_2+i+j,m_2+k+i;m_2+k+i+1;-\beta_2\mu^2\right]
\end{aligned}
\tag{15}
$$

Based on the definition of the AFD in [24], we have the expression of AFD as

$$
AFD(\mu) = \frac{\Pr(R_1<\mu)}{LCR(\mu)} = \frac{T_sF_{R_1}(\mu)}{F_{R_1}(\mu)-F_{R_1,R_2}(\mu,\mu)} \tag{16}
$$

Similar as (15), (16) can be calculated.

5 Numerical Results and Discussion

In this section, we will present various numerical and simulation results under different correlated Fisher–Snedecor $\mathcal{F}$ fading and shadowing scenarios based on the previous derived analytical expressions. In simulation, we adopted the simulation method described in [26] to generate two correlated Nakagami-m variables and their inverse variables with arbitrary fading parameters. The simulations that are obtained via generating 10^6 iterations are compared with the analytical results. Simulation results matched well with the numerical analysis and verify the accuracy of our derivations. In these figures, the lines represent the numerical analysis and the circle marks stand for the simulated results.

Firstly, we show the OP as a function of the average SNR with the outage threshold $\gamma_{th} = 3$ dB over correlated $\mathcal{F}$ composite fading channels in Fig. 1. In numerical analysis and simulation, seven different combinations of the multipath parameters (m_1 and m_2), the shadowing parameters (n_1 and n_2) and the correlation coefficients (ρ_G and ρ_N) are considered. It can be seen from Fig. 1 that the OP gets better as the m-parameters increases with the same shadowing parameters ($n_1 = 5, n_2 = 6$) and the same correlation coefficients ($\rho_G = \rho_N = 0.5$) by comparing the red line (where the dash line denotes $m_1 = 0.5$ and $m_2 = 0.8$, the dot line denotes $m_1 = 2$ and $m_2 = 3$) with the black line ($m_1 = 1.2$ and $m_2 = 1.5$ as a benchmark). It is because the small scale fading has impact on the slope of the OP performance, namely, the lager the value of m, the lager the curve slope. On the other hand, the shadowing parameters and the correlation coefficients have impact on the coding gain of the OP performance in high SNR region, where the coding gain is considered as the shift degree of OP or bit (symbol) error rate line to the left versus SNR in a log-log scale. When the shadowing parameter n gets larger from heavy shadowing to light shadowing, the code gain

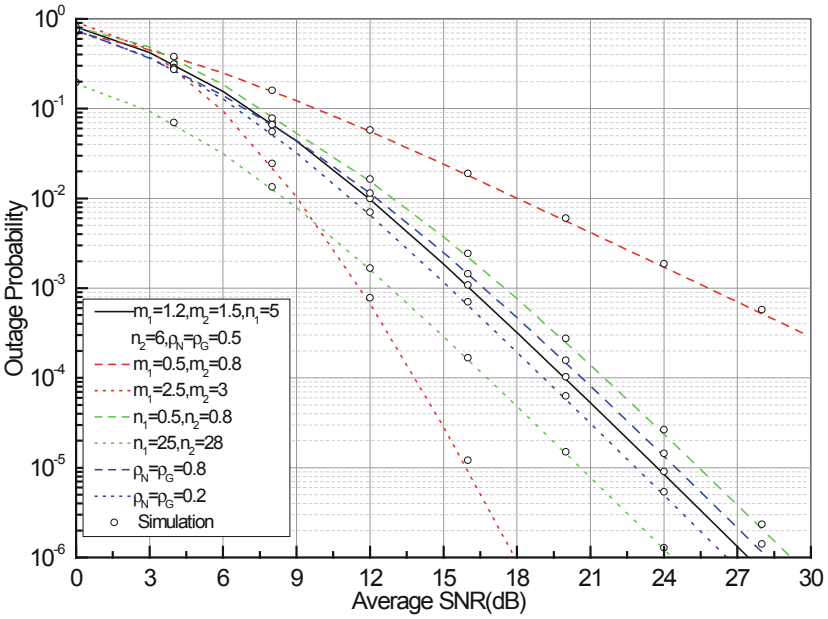

Fig. 1. Outage probability of the dual-branch SC system as a function of the average SNR with $\gamma_{th} = 3$ dB over correlated $\mathcal{F}$ composite fading channels (Color figure online)

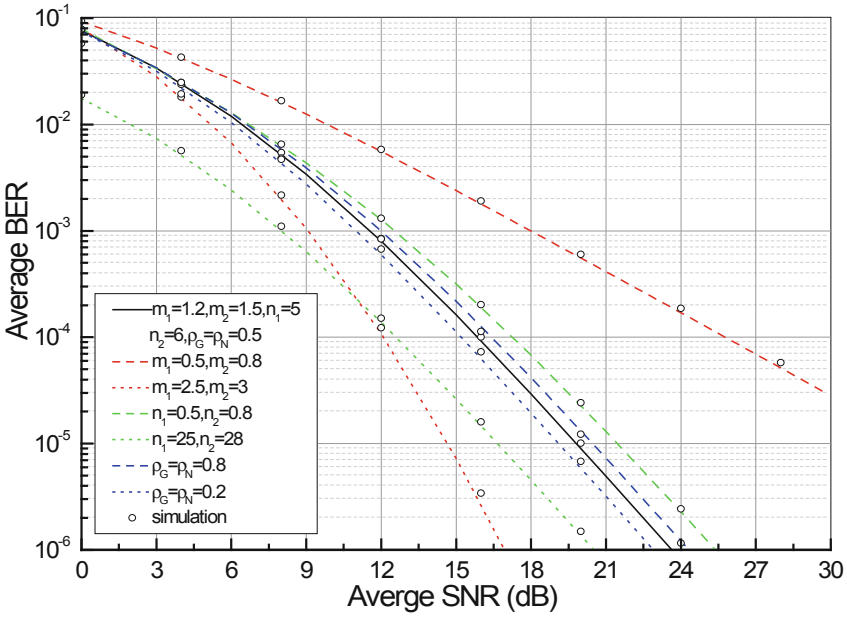

Fig. 2. Average BER of DPSK of the dual-branch SC system as a function of the average SNR over correlated $\mathcal{F}$ composite fading channels (Color figure online)

increases by comparing the green line (where the dash line denotes $n_1 = 0.5$ and $n_2 = 0.8$, the dot line denotes $n_1 = 25$ and $n_2 = 28$) with the black line ($n_1 = 5$ and $n_2 = 6$ as a benchmark), where the other parameters keep the same as those of the benchmark line. However, the code gain changes less as the correlation coefficients decrease by comparing the blue line (where the dash line denotes $\rho_G = \rho_N = 0.2$, the dot line denotes $\rho_G = \rho_N = 0.8$) with the black line ($\rho_G = \rho_N = 0.5$ as a benchmark) in Fig. 1.

Secondly, in Fig. 2, we illustrate the average BER of DPSK as a function of the average SNR with the same parameters as those used in Fig. 1. As expected, this figure also confirms our results that is shown in Fig. 1.

Thirdly, Fig. 3 demonstrates the LCR · *Ts* as a function of the specified lever μ with $\Omega_i = 1 (i = 1, 2)$ in the moderate shadowing scenarios. As it was expected, when the value of m increases, the LCR decreases by comparing the green line with the black line (as a benchmark) in Fig. 3, which shows that fades take place less frequently. Moreover, the shape of LCR gets narrower and falls rapidly on both sides as the value of m increases. This is because m characterizes the fast fading of the instantaneous signal envelope. On the contrary, the correlation coefficients show less effect on the LCR at lower threshold levels whereas the LCR decreases as the correlation coefficients grows at higher threshold levels. In Fig. 4, the ADF/*Ts* is plotted under the same scenarios as Fig. 3. Since LCR and AFD are inversely proportional, some similar conclusions can be also obtained. It is interesting that these curves show a floor effect at lower threshold levels.

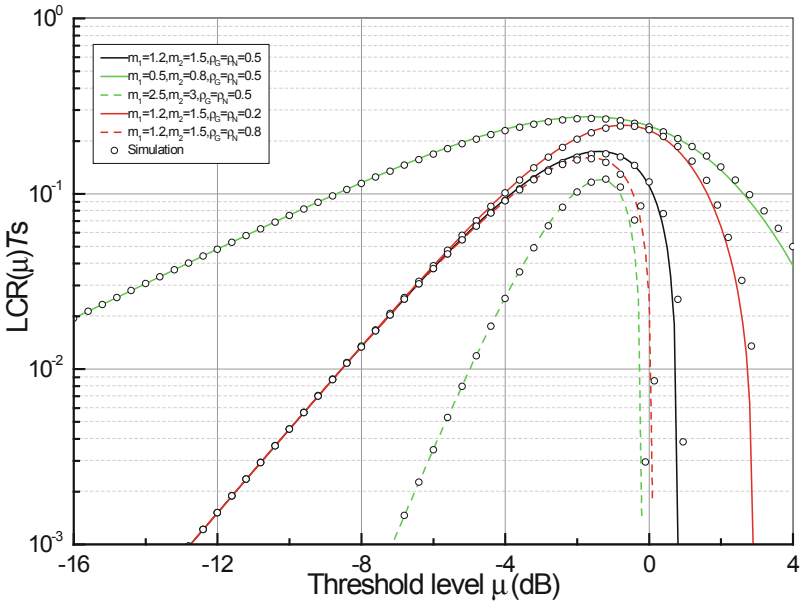

Fig. 3. LCR · *Ts* of the sampled correlated $\mathcal{F}$ composite fading envelope as a function the specified threshold lever μ with $\Omega_i = 1, n_1 = 5, n_2 = 6$ (Color figure online)

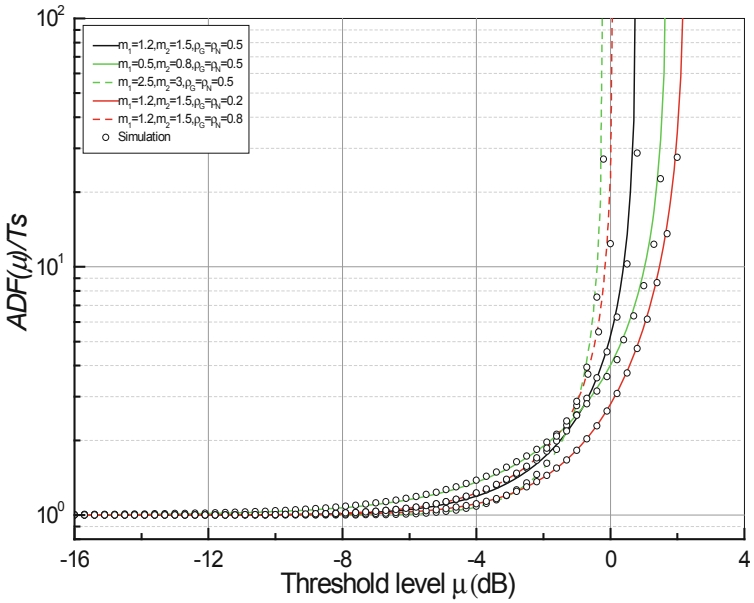

Fig. 4. ADF/*Ts* of the sampled correlated $\mathcal{F}$ composite fading envelope as a function the threshold lever u with $\Omega_i = 1, n_1 = 5, n_2 = 6$ (Color figure online)

6 Conclusions

In this paper, we investigated a correlated Fisher–Snedecor $\mathcal{F}$ composite distribution with arbitrary fading parameters. The novel theoretical representations including the bivariate PDF, the bivariate CDF, the joint moments and the power correlation coefficient for this distribution were derived. Based on the bivariate CDF, we analyzed the OP and the BER of different binary digital modulation schemes for a correlated dual-branch selection diversity receiver and evaluated the LCR and the AFD of a sampled Fisher-Snedecor $\mathcal{F}$ composited fading envelope. Simulation results matched well with the numerical analysis and verified the validity of the theoretical expressions under various correlated fading and shadowing scenarios.

References

1. Yoo, S.K., Cotton, S.L., Sofotasios, P.C., Matthaiou, M., Valkama, M., Karagiannidis, G.K.: The Fisher-Snedecor $\mathcal{F}$ distribution: a simple and accurate composite fading model. IEEE Commun. Lett. **21**(7), 1661–1664 (2017)
2. Badarneh, O.S., da Costa, D.B., Sofotasios, P.C., Muhaidat, S., Cotton, S.L.: On the sum of Fisher-Snedecor $\mathcal{F}$ variates and its application to maximal-ratio combining. IEEE Wirel. Commun. Lett. **7**(6), 966–969(2018)
3. Kong, L., Kaddoum, G.: On physical layer security over the Fisher-Snedecor $\mathcal{F}$ wiretap fading channels. IEEE Access **6**, 39466–39472 (2018)

4. Yoo, S.K, Sofotasios, P.C., Cotton, S.L., et al.: A comprehensive analysis of the achievable channel capacity in $\mathcal{F}$ composite fading channels. IEEE Access **7**, 34078–34094 (2019)
5. Yoo, S.K., Sofotasios, P.C., Cotton, S.L., Muhaidat, S., Badarneh, O.S., Karagiannidis, G. K.: Entropy and energy detection-based spectrum sensing over $\mathcal{F}$-composite fading channels. IEEE Trans. Commun. **67**(7), 4641–4653 (2019)
6. Al-Hmood, H., Al-Raweshidy, H.S.: Selection combining scheme over non-identically distributed Fisher-Snedecor $\mathcal{F}$ fading channels. arXiv:1905.05595 (2019)
7. Zhao, H., Yang, L., Salem, A.S., Alouini, M.: Ergodic capacity under power adaption over Fisher-Snedecor $\mathcal{F}$ fading channels. IEEE Commun. Lett. **23**(3), 546–549 (2019)
8. Chen, S., Zhang, J., Karagiannidis, G.K., Ai, B.: Effective rate of MISO systems over Fisher-Snedecor $\mathcal{F}$ fading channels. IEEE Commun. Lett. **22**(12), 2619–2622 (2018)
9. Aldalgamouni, T., Ilter, M.C., Badarneh, O.S., Yanikomeroglu, H.: Performance analysis of Fisher-Snedecor $\mathcal{F}$ composite fading channels. In: 2018 IEEE Middle East and North Africa Communications Conference (MENACOMM), pp. 1–5, IEEE, Jounieh (2018)
10. Reig, J., Rubio, L., Cardona, N.: Bivariate Nakagami-m distribution with arbitrary fading parameters. Electron. Lett. **38**(25), 1715–1717 (2002)
11. Zhang, R., Wei, J., Michelson, D.G., Leung, V.C.M.: Outage probability of MRC diversity over correlated shadowed fading channels. IEEE Wirel. Commun. Lett. **1**(5), 516–519 (2012)
12. Bithas, P.S., Sagias, N.C., Mathiopoulos, P.T., Kotsopoulos, S.A., Maras, A.M.: On the correlated K-distribution with arbitrary fading parameters. IEEE Sig. Process Lett. **15**, 541–544 (2008)
13. Bithas, P.S., Sagias, N.C., Mathiopoulos, P.T.: The bivariate generalized-K (K_G) distribution and its application to diversity receivers. IEEE Trans. Commun. **57**(9), 2655–2662 (2009)
14. Reddy, T., Subadar, R., Sahu, P.R.: Outage probability of selection combiner over exponentially correlated Weibull-gamma fading channels for arbitrary number of branches. In: 2010 National Conference on Communications, pp. 1–5, IEEE, Madras (2010)
15. Ni, Z., Zhang, X., Liu, X., Yang, D.: Bivariate Weibull-gamma composite distribution with arbitrary fading parameters. Electron. Lett. **48**(18), 1165–1167 (2012)
16. Trigui, I., Laourine, A., Affes, S., Stéphenne, A.: Bivariate $\mathcal{G}$ distribution with arbitrary fading parameters. In: 2009 3rd International Conference on Signals, Circuits and Systems (SCS), pp. 1–5, IEEE, Medenine (2009)
17. Reig, J., Rubio, L., Rodrigo-Peñarrocha, V.M.: On the bivariate Nakagami-lognormal distribution and its correlation properties. Int. J. Antennas Propag. **2014**, 1–8 (2014)
18. Gradshteyn, I., Ryzhik, I.: Table of Integrals, Series, and Products, 8th edn. Academic Press, London (2007)
19. Chun, Y.J., Cotton, S.L., Dhillon, H.S., Lopez-Martinez, F.J., Paris, J.F., Yoo, S.K.: A comprehensive analysis of 5G heterogeneous cellular systems operating over $\kappa - \mu$ shadowed fading channels. IEEE Trans. Wirel. Commun. **16**(11), 6995–7010 (2017)
20. Simon, M.K., Alouni, M.-S.: Digital Communication over Fading Channels, 2nd edn. Wiley, New York (2005)
21. Ansari, I.S., Al-Ahmadi, S., Yilmaz, F., Alouini, M., Yanikomeroglu, H.: A new formula for the BER of binary modulations with dual-branch selection over generalized-K composite fading channels. IEEE Trans. Commun. **59**(10), 2654–2658 (2011)
22. Wojnar, A.H.: Unknown bounds on performance in Nakagami channels. IEEE Trans. Commun. **34**(1), 22–24 (1986)
23. García-Corrales, C., Canete, F.J., Paris, J.F.: Capacity of $\kappa - \mu$ shadowed fading channels. Int. J. Antennas Propag. **2014**, 1–8 (2014)

24. López-Martínez, F.J., Martos-Naya, E., Paris, J.F., Fernández-Plazaola, U.: Higher order statistics of sampled fading channels with applications. IEEE Trans. Veh. Technol. **61**(7), 3342–3346 (2012)
25. López-Fernández, J., Paris, J.F., Martos-Naya, E.: Bivariate Rician shadowed fading model. IEEE Trans. Veh. Technol. **67**(1), 378–384 (2018)
26. Reig, J., Martinez-Amoraga, M.A., Rubio, L.: Generation of bivariate Nakagami-m fading envelopes with arbitrary not necessary identical fading parameters. Wirel. Commun. Mob. Comput. **2007**(7), 531–537 (2007)